



Research article

Optimization of the processing technology of schizonepetae herba carbonisata using response surface methodology and artificial neural network and comparing the chemical profiles between raw and charred schizonepetae herba by UPLC-Q-TOF-MS



Xiaoying Ding^{a,1}, Huaiyou Wang^{b,1}, Hengyang Li^a, Tao Wang^a, Shenghui Hao^a, Wenjie Li^a, Chengyue Wang^a, Lei Wang^{a,c}, Yuguang Zheng^{a,d}, Qi An^{a,e,***}, Long Guo^{a,c,**}, Dan Zhang^{a,c,*}

^a Traditional Chinese Medicine Processing Technology Innovation Centre of Hebei Province, College of Pharmacy, Hebei University of Chinese Medicine, Shijiazhuang 050200, China

^b College of Pharmacy, Henan University, Kaifeng 475004, China

^c International Joint Research Centre on Resource Utilization and Quality Evaluation of Traditional Chinese Medicine of Hebei Province, Shijiazhuang, 050200, China

^d Hebei Chemical and Pharmaceutical College, Shijiazhuang 050026, China

^e Department of Chinese Materia Medica, Hebei Institute for Drug and Medical Device Control, Shijiazhuang, 050200, China

ARTICLE INFO

Keywords:

Schizonepetae herba
Schizonepetae herba carbonisata
Response surface methodology
Artificial neural network
Ultra performance liquid chromatography/
quadrupole time-of-flight mass spectrometry

ABSTRACT

In this study, response surface methodology (RSM) and artificial neural network (ANN) were used to predict and validate the optimal processing method of Schizonepetae Herba Carbonisata (SHC). The highest overall desirability (OD) value of the total flavonoids content (TFC), total tannin content (TTC), and adsorption capacity (AC) were used as response values. The optimal processing technology processing time lasted 10 min at a processing temperature of 178 °C and the herbs/machine had a volume of 77 g/5 L. The Ultra Performance Liquid Chromatography/Quadrupole Time-of-Flight Mass Spectrometry (UPLC-Q-TOF-MS), combined with chemometrics, was used to investigate the changes of compounds in Schizonepetae Herba (SH) before and after being charred. A total of 104 compounds were tentatively identified in SH and 83 in SHC. Fifteen differential compounds were found between by chemometrics SH and SHC. Altogether, our findings can provide a practical approach to the processing technology of carbonizing by stirring SH.

* Corresponding author. Traditional Chinese Medicine Processing Technology Innovation Centre of Hebei Province, College of Pharmacy, Hebei University of Chinese Medicine, Shijiazhuang 050200, China

** Corresponding author. Traditional Chinese Medicine Processing Technology Innovation Centre of Hebei Province, College of Pharmacy, Hebei University of Chinese Medicine, Shijiazhuang 050200, China

*** Corresponding author. Traditional Chinese Medicine Processing Technology Innovation Centre of Hebei Province, College of Pharmacy, Hebei University of Chinese Medicine, Shijiazhuang 050200, China

E-mail addresses: qianid2022@163.com (Q. An), guo_long11@163.com (L. Guo), zhangdan@hebcm.edu.cn (D. Zhang).

¹ These authors contributed equally to this work.

<https://doi.org/10.1016/j.heliyon.2023.e13398>

Received 3 November 2022; Received in revised form 25 January 2023; Accepted 30 January 2023

Available online 2 February 2023

2405-8440/© 2023 The Authors. Published by Elsevier Ltd. This is an open access article under the CC BY-NC-ND license (<http://creativecommons.org/licenses/by-nc-nd/4.0/>).

1. Introduction

Processing of Chinese medicine is a unique pharmaceutical technique based on the theory of Chinese medicine, clinical application needs and the nature of Chinese medicine, as well as the blending and preparations. Through processing, drugs can achieve the effects of reducing toxicity and increasing efficacy, changing medicinal properties, inducing medicine into the meridian, and correcting the taste to meet different therapeutic needs. Stir-baking until charred is a common method of processing herbs. Charred decoction pieces have been used in China to stop bleeding for more than 2000 years. The hemostatic effect of charred decoction pieces can be roughly divided into two categories: one in which it does not have any hemostatic effect itself and is used to stop bleeding after being processed, and one in which its hemostatic effect is enhanced after being processed. Ge (an ancient Chinese medical scientist) said “if the blood is hot, it moves; if it is cold, it clots; if it is black, it stops” [1]. This is the original theory of “stopping bleeding when red is seen” and “stopping bleeding by frying charcoal” in later times.

Schizonepetae Herba (SH) is the dried aerial part of *Schizonepeta tenuifolia* Briq. In the Lamiaceae family, and Schizonepetae Herba Carbonisata (SHC) is a processed product of SH. SH was first reported in *Shennong Ben Cao Jing* (a book written 2000 years ago) for its ability to dispel the common cold, pathogenic “wind evils” and promote allergic dermatitis [2]. In the *Ben Cao Gang Mu* (a book published 400 years ago), it is recorded that SHC can be used to treat bloody stools and allergic reactions [3]. Various forms of SH have been found to have anti-inflammatory, antioxidant, analgesic, anti-tumour, and immunomodulatory effects, and have been used to successfully treat symptoms such as fever, colds, respiratory infections, and allergic dermatitis. While SHC has significant hemostatic effects, it has long been used in treating bloody stools and allergies [4]. The above effects are likely related to the volatile oils, flavonoids, organic acids, and monoterpenoids contained in SH [5]. Due to its prominent bioactivities, it is necessary to develop a quantifiable processing method for SHC.

Response surface methodology (RSM) has widely been used in analyzing a variety of biological processes, designing experiments, building models, evaluating the effects of different factors, and optimizing conditions at present [6]. Artificial neural networks (ANNs) are inspired by the human central nervous system, in which a vestigial network of neurons is interconnected and can compute the input information [7]. ANNs can effectively handle nonlinear relationships, even when the exact nature of the relationship is unknown, giving it an outstanding advantage [8]. ANNs have emerged as a superior alternative to RSM due to their ability to compute complex decision processes. In addition, RSM and ANNs have been widely used in extracting active ingredients and processing technology in plants and Chinese medicine. Optimizing of kidney bean antioxidants [9], extracting polysaccharides from *Lilium lancifolium* Thunb via ultrasound-assisted aqueous two-phase extraction [10], and infusing bioactive components from laver being via ultrasound-assisted extraction [11] are a few examples of this process. In addition, it was found that ANN provided better predictability and greater accuracy. Applying the optimization of the processing technology of traditional Chinese medicine with RSM and ANN has begun to be attempted, with honey-roasted Chuanxiong Rhizome as a typical case [12]. The obtained processing technology is stable, and the model prediction effect is good. RSM and ANN models have not been compared regarding the prediction of SHC processing technology to the best of our knowledge.

Although SHC has been used for more than 600 years as a hemostatic drug [13], very little information is available for discussion concerning its processing technology. Therefore, the first objective of the present study is to obtain the optimal processing technology for SHC. The second objective is to investigate the changes of compounds in SH before and after it is charred. To optimize the SHC processing technology, RSM and ANN models were developed and the total flavonoids content (TFC), total tannin content (TTC), and adsorption capacity (AC) were selected as response values. The optimal conditions for carbonation processing were predicted and validated by RSM and ANN models. A comprehensive analysis of SH and SHC was performed using UPLC-Q-TOF-MS to investigate the chemical composition changes in SH before and after being charred. Chemometric methods were then performed to identify differential compounds between SH and SHC samples.

2. Material and methods

2.1. Materials and reagents

14 batches of SH were collected from different areas in China (Table S1). The voucher specimens were identified by Dr. Dan Zhang and deposited in the Traditional Chinese Medicine Processing Technology Innovation Centre of Hebei Province, Hebei University of Chinese Medicine.

Rutin (lot number: 1009H021, >98%) was purchased from Beijing Solarbio Technology Co., Ltd. (Beijing, China). Gallic acid (lot number: PRF7091941, >98%) was purchased from Chengdu Pusi Bio-Technology Co., Ltd. (Chengdu, China). LC-MS grade methanol, acetonitrile, and formic acid were purchased from Fisher Scientific (Pittsburgh, PA, USA). Ultrapure water was prepared by a Synergy water purification system (Millipore Corp, Billerica, MA, USA). All other reagents and solvents were of analytical grade.

2.2. Optimization of processing technology of SHC

2.2.1. Sample preparation

The condition of the total flavonoids and total tannins extracts of SHC were determined by RSM in a preliminary experiment. All samples were sifted through 60 mesh, for the total flavonoids, according to the solvent/sample ratio of 15 (mL/g), 50% ethanol, and ultrasonic (Jp-060s ultrasonic bath, Shenzhen, China) at ~30 °C for 10 min. For the total tannin, according to a solvent/sample ratio of 25 (mL/g), 39% ethanol, and ultrasonically at ~30 °C for 91 min. These were centrifuged twice using a high-speed centrifuge

(Eppendorf Centrifuge 5418, Shanghai, China) at 13,000 rpm. The SHC extract was stored at 4 °C for use in future experiments.

2.2.2. Determination of total flavonoids

The TFC was determined according to the aluminum chloride colorimetric assay [14]. 0.2 mL of the solution was added to a 10 mL volumetric flask, and mixed with 0.3 mL of 5% NaNO₂ for 6 min. 0.3 mL of 10% AlCl₃ was added, shaken well and left for another 6 min. The reaction stopped when it reached 4 mL of 4% NaOH and deionized water was used to fix the volume to the scale. After being incubated at room temperature for 15 min, the reaction mixture absorbance was measured at 514 nm against a deionized water blank on a Multimode Microplate Reader (PerkinElmer Victor Nivo, MA, USA). Rutin was chosen as a standard. The correlation equation constructed with rutin (0–0.016 mg/mL) was $A = 6.2621C - 0.0027$ ($R^2 = 0.9997$). The TFC was expressed as mg of rutin equivalents per gram of dry weight. All samples were analyzed in triplicate.

2.2.3. Determination of total tannins

The amount of tannins in the SHC extract was determined with slight modifications to the Folin-Ciocalteu method [15]. 0.5 mL of the SHC extract was added to a brown 25 mL volumetric flask. 0.5 mL of the Folin–Ciocalteu reagent, 2.5 mL of deionized water, and 29% Na₂CO₃ was used to fix the volume to the scale. The mixture was shaken well and kept at room temperature for 30 min. The reaction mixture absorbance was measured at 760 nm against a deionized water blank on a Multimode Microplate Reader (PerkinElmer Victor Nivo, MA, USA). Gallic acid was chosen as a standard. The correlation equation constructed with gallic acid (0–0.037 mg/mL) was $A = 50.723C - 0.0615$ ($R^2 = 0.9996$). The TTC was expressed as mg of gallic acid equivalents per gram of dry weight. All samples were analyzed in triplicate.

2.2.4. Determination of adsorption capacity

The AC of SHC was determined by the test methods of wooden activated carbon–determination of methylene blue absorption (the State Standard of the People's Republic of China GB/T12496.10–1999) [16].

The preparation of the methylene blue standard solutions was as follows: 0.17 g of methylene blue containing 0.049% water was added to a 100 mL volumetric flask and phosphate buffer solution with a pH of 7 was used to fix the volume to the scale with a concentration of 1.70 mg/mL. This was diluted to 0.024 mg/mL with a phosphate buffer solution of pH 7.

0.01 mg of SHC samples (sifted through 60 mesh) were added to 2 mL of 0.019 mg/mL methylene blue and then put on the thermostat oscillator at 25 °C at 300 rpm for 40 min. It was then centrifuged for 10 min (13,000 rpm). The reaction mixture absorbance was measured at 665 nm against a phosphate buffer solution blank with a pH of 7 on a Multimode Microplate Reader (PerkinElmer Victor Nivo, MA, USA). Methylene blue was chosen as a standard. The correlation equation constructed with methylene blue (0–0.024 mg/mL) was $A = 26.955C + 0.0288$ ($R^2 = 0.9991$). The AC was expressed as mg of methylene blue equivalents per gram of dry weight. All samples were analyzed in triplicate.

2.2.5. Experimental design of RSM

The total score of TFC, TTC, and AC was normalized as evaluation indexes to optimize the best processing technology for SHC. A single factor experimental design was first used to analyze various processing parameters of SHC, including processing time (5, 10, 15, and 20 min), and temperature (140, 180, 220, and 260 °C), and the herbs/machine volume (10, 70, 130 and 190 g/5 L) were optimized. The normalization method was as follows:

$$d_n = (d_i - d_{min}) \div (d_{max} - d_{min}) \quad (1)$$

where d_i , d_{min} , and d_{max} are the actual values measured in the experiment, d_{min} and d_{max} are the minimum and maximum values of the set of values, respectively. d_n is the normalized value of d_i . The normalized value of each index was calculated according to the formula to calculate the geometric mean and obtain the overall desirability value (OD) [17]. This was calculated as follows:

$$OD = (d_1 d_2 d_3 \dots d_n)^{1/n} \quad (2)$$

n is the number of indicators [18].

The Box-Behnken design (BBD) was used to achieve further optimization of the SHC processing technology. The RSM was designed based on the results of single-factor experiments. Twelve experiments were enhanced with five replications to assess the pure error to afford a BBD that consisted of 17 runs, with each one being evaluated at three different levels (−1, 0, +1). The independent variables, levels, and experimental design were all ranked in coded and decoded terms (Table S2). The runs were performed in a random order. The OD was set as the response to the design experiments. The experimental orders, levels of variables, and response values were summarized in Table 1. Data pertaining to three independent variables and one response variable were analyzed to get a second-order polynomial model as follows:

$$Y = b_0 + \sum_{i=1}^3 b_i X_i + \sum_{i=1}^3 b_{ii} X_{ii} + \sum_{i < j}^3 b_{ij} X_i X_j \quad (3)$$

where b_0 , b_i , b_{ii} , and b_{ij} ($i \neq j$) are the regression coefficients for intercept, linear, quadratic, and interaction terms, respectively, X_i and X_j are the independent variables. Design-Expert (Version 8.0.6; Stat-Ease Inc., Minneapolis, MN, USA) was used for statistical analysis. The quality of the fit of the polynomial model was evaluated with respect to the coefficient of determination (R^2) and the F -test. The

Table 1

Summary design matrix for investigated responses.

Standard order ^a	Run order ^b	A: Processing time (min)	B: Processing temperature (°C)	C: Weight of medicinal herbs (g)	d ₁ : Extraction rate of total flavonoids (mg/g)	d ₂ : Extraction rate of total tannin (mg/g)	d ₃ : Adsorption capacity (mg/g)	Response (OD)		
								Experimental data	RSM predicted	ANN predicted
7	1	5	180	130	0.0183	0.2392	0.2385	0.1015	0.1468	0.1052
1	2	5	140	70	0.0296	0.0340	0.2226	0.0607	-0.0116	0.1813
9	3	10	140	10	0.4893	0.0000	0.2385	0.0000	0.0833	-0.0608
10	4	10	220	10	0.0068	0.1803	0.0000	0.0000	-0.0271	0.0069
5	5	5	180	10	0.1041	0.0986	0.5723	0.1805	0.1696	0.1618
4	6	15	220	70	0.0000	0.3129	0.2067	0.0000	0.0723	0.0000
3	7	5	220	70	0.0281	0.3333	0.2544	0.1336	0.1715	0.1464
17	8	10	180	70	0.7124	0.9116	0.9677	0.8566	0.9349	0.9318
11	9	10	140	130	0.1322	0.1088	0.0954	0.1111	0.1382	0.1113
6	10	15	180	10	0.1802	0.1908	0.1749	0.1818	0.1365	0.1804
13	11	10	180	70	0.9355	0.9762	0.9984	0.9697	0.9349	0.9318
2	12	15	140	70	0.3256	0.4456	0.3339	0.3645	0.3266	0.2751
16	13	10	180	70	1.0000	0.9660	0.9571	0.9742	0.9349	0.9318
14	14	10	180	70	0.9289	1.0000	0.9968	0.9747	0.9349	0.9318
12	15	10	220	130	0.1874	0.2704	0.3498	0.2607	0.1775	0.2603
15	16	10	180	70	0.7636	0.9524	1.0000	0.8993	0.9349	0.9318
8	17	15	180	130	0.3802	0.3118	0.5723	0.4078	0.4188	0.3431

^a Randomized.^b Not randomized.

lack of a fit *F*value ($p < 0.05$) was acquired by an analysis of variance (ANOVA) and used to demonstrate variable significance and model adequacy. The optimal processing conditions for prediction were verified by experiments to verify the prediction ability and sufficiency of the model.

2.2.6. ANN model

RSM-based data were applied to the feed of the network through the deep learning Toolbox of MATLAB R2020a (MathWorks, Inc. MA, USA). The ANN was used to predict a nonlinear relationship between the input parameters (X_1 , X_2 , X_3) and output response (Y). The multilayer perceptron (MLP) and backpropagation feed-forward (BPFF) model were used in the nonlinear analysis to predict independent and dependent variables [19]. The ANN model is comprised of three independent variables X_1 , X_2 , X_3 (processing time, processing temperature, quantity of reagent) and one dependent variable, Y (OD). Seventeen samples were apportioned for training (70% of datasets), validation (15% of datasets), and testing (15% of datasets) to validate and test the data. According to the approximation of the mean square error (MSE) function, five hidden neurons were set in the process model, and the network with the minimum MSE and the maximum R^2 the ANN model selected to run.

2.3. UPLC and UPLC-Q-TOF-MS detection

2.3.1. Sample preparation

Fourteen batches of dried SH were processed into SHC by a type-5 stir-frying machine (5 L of volume. Changzhou Maisi Machinery Co., Ltd., Changzhou, China) according to optimal conditions. Dried SH and SHC were then turned into a powder of a homogeneous size (sifted through 60 mesh). An aliquot of the sample powder was immersed according to the solvent/material ratio of 15 (mL/g), 50% ethanol, followed by ultrasonic extraction at 30 °C for 10 min. Before analysing UPLC and UPLC-Q-TOF-MS, extracts were centrifuged twice at 13,000 rpm for 10 min and then filtered through a 0.22 µm nylon membrane. Before analysing UPLC-Q-TOF-MS, rutin was added at a concentration of 0.2065 mg/mL, following 100 µL of a rutin concentration mixed with 900 µL of the sample solution.

2.3.2. UPLC and UPLC-Q-TOF-MS condition

The UPLC analysis was performed on a Waters ACQUITY UPLC H-Class system (Waters Technology Co., Ltd, Milford, MA, USA). Chromatographic separation was conducted on a Waters ACQUITY UPLC® HSS T₃ column (2.1 × 100 mm, 1.8 µm, Waters Technology Co., Ltd, Milford, MA, USA). The mobile phase consisted of 0.1% formic acid in water (A) and acetonitrile (B) with gradient elution as follows: 0–6 min, 15–19% B; 6–10 min, 19–20% B; 10–14 min, 20–25% B; 14–20 min, 25–30% B; 20–23 min, 30–100%. The flow rate was 0.3 mL/min, the column temperature was 30 °C, the injection volume was 2 µL and the detection wavelength was 283 nm.

The UPLC-Q-TOF-MS analysis was performed on an Agilent 1290 UPLC system coupled with an Agilent 6545 quadrupole time-of-flight mass spectrometer system (Agilent Technologies, Santa Clara, CA, USA). Chromatographic separation was also performed on a Waters ACQUITY UPLC® HSS T₃ column (2.1 × 100 mm, 1.8 µm). The binary gradient elution system consisted of water containing 0.1% formic acid (A) and acetonitrile (B). The gradient elution condition was as follows: 0–8 min, 15–19% B; 8–14 min, 19–20% B; 14–18 min, 20–25% B; 18–25 min, 25–30% B; 25–28 min, 30–100%. Injection volume: 0.8 µL. The flow rate and column temperature were the same as for the UPLC analysis. The MS acquisition parameters were as follows: the drying gas (N₂) temperature was 320 °C; the sheath gas temperature was 350 °C; the drying gas (N₂) flow rate was 10.0 L/min; the sheath gas flow (N₂) rate was 11 L/min; the nebulizer gas pressure was 35 psi; the capillary voltage was 4000 V; the fragmentor voltage was 135 V; the collision energy was 20 eV and 40 eV. The analysis was operated in positive mode with the mass range of m/z 100–1700 Da. Data acquisition was conducted on MassHunter Workstation (Agilent Technologies, Santa Clara, CA, USA).

2.3.3. Establishment and evaluation of UPLC fingerprints

The precision, repeatability, and stability of the UPLC method were validated to ensure the reliability of the UPLC method for SH and SHC samples. Using the Similarity Evaluation System of Chromatographic Fingerprint of Traditional Chinese Medicine (version 2004 A), the UPLC fingerprints of SH and SHC samples were automatically matched. The median method was used to form a reference fingerprint by comparing the chromatograms of 14 batches of SH and SHC samples. The similarity of the reference fingerprint to the chromatograms of different SH and SHC samples was calculated.

2.4. Statistical analysis

Each experiment was carried out in triplicate with three replicas in each case. Experimental data were expressed as means ± standard deviation (SD). The LC-MS data acquisition was conducted on MassHunter Workstation (Agilent Technologies, Santa Clara, CA, USA). Identification of compounds in SH and SHC were based on the data of literature information and metabolite databases (Chemspider, MassBank, and Agilent herbal library-v20-04-17). The dataset was introduced into SIMCA software (version 13.0, Umetrics, Umea, Sweden) for principal component analysis (PCA) and orthogonal partial least-squares principal discriminant analysis (OPLS-DA) after normalization occurred. Mean ± SD was performed using SPSS software (version 22.0; IBM, Armonk, NY, USA).

3. Results and discussion

3.1. Optimization of processing technology of SHC

3.1.1. Determination of total flavonoids, total tannins, and adsorption capacity method validation

The linearity, precision, repeatability, stability, and accuracy of the established method were evaluated to determine the TFC, TTC, and AC. As shown in Table S3, all calibration curves had good linearity with high correlation coefficients ($r^2 \geq 0.9990$) over the tested range. The relative standard deviations (RSDs) of intra- and inter-day precisions were less than 0.17%, 1.99%, 0.51% and 0.57%, 2.10%, 1.21%. The RSDs of repeatability were under 1.47%, 1.29%, and 0.27%, while stability was under 1.28%, 1.62%, and 0.48%. The overall recoveries of the three indicators were between 97.18 and 99.23%, and the RSD was less than 1.85%. According to the results, the established method was capable of analyzing SHC samples.

3.1.2. Single factor experiment

As shown in Fig. S1, when the treatment time was increased from 5 to 10 min, the OD increased from 10% to 20% with time and then decreased with time. From 140 °C to 180 °C, the OD increased significantly and it started to decrease from 180 °C to 260 °C. When the herbs/machine volume is between 10 g/5 L and 190 g/5 L, the maximum OD was 70 g/5 L. For this reason, 10 min of processing

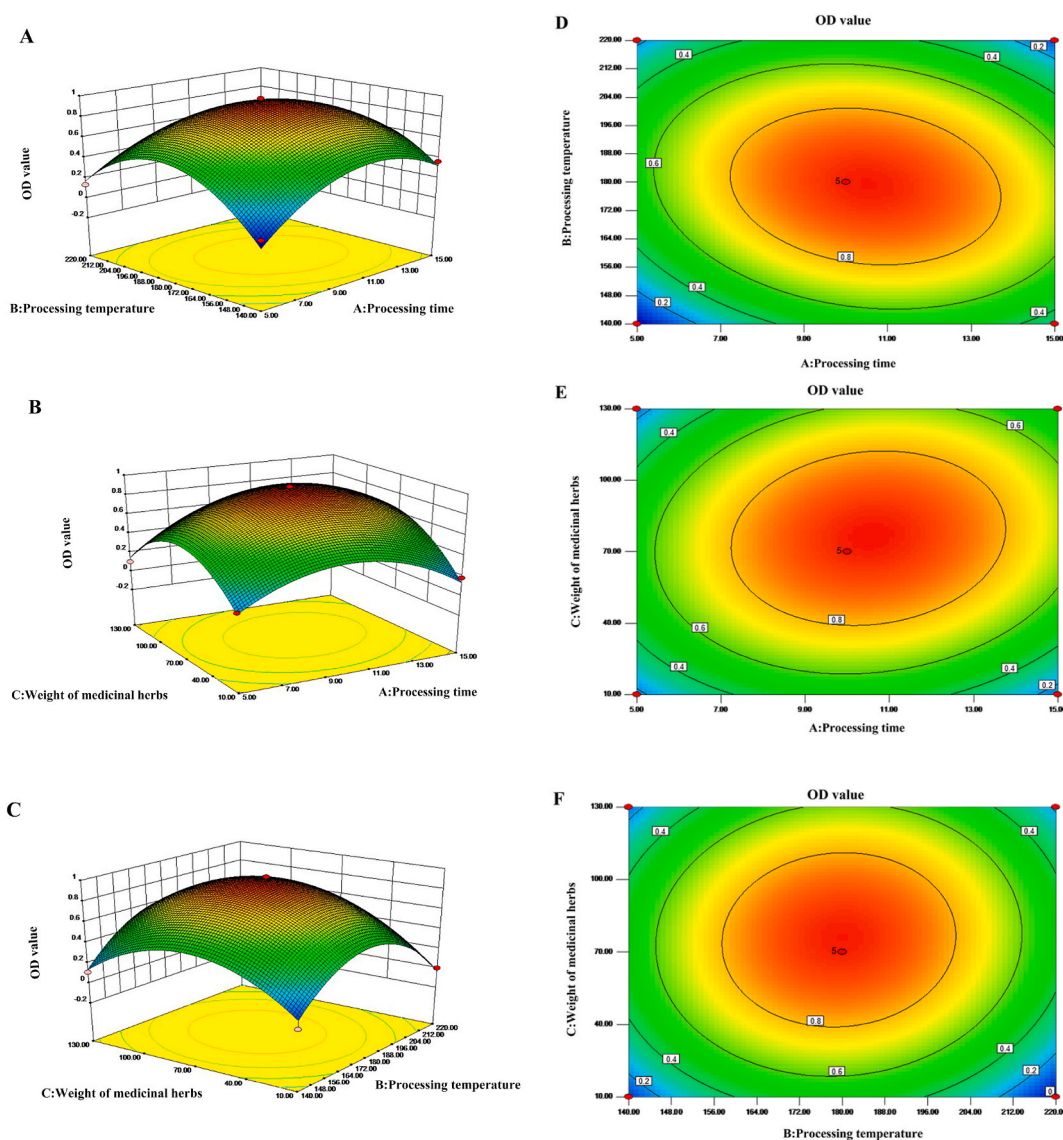
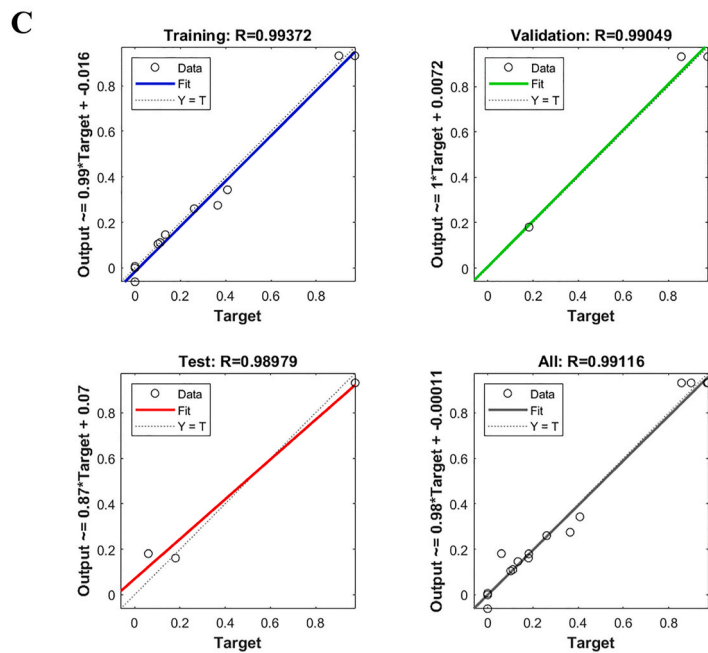
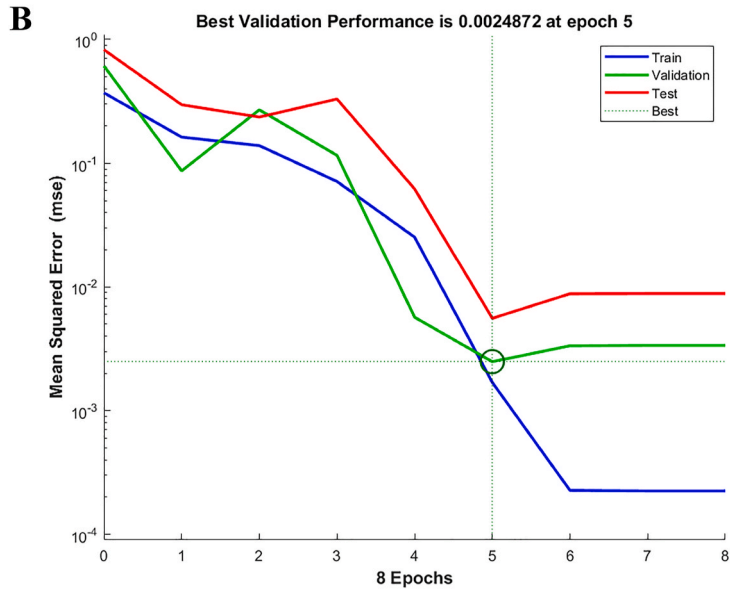
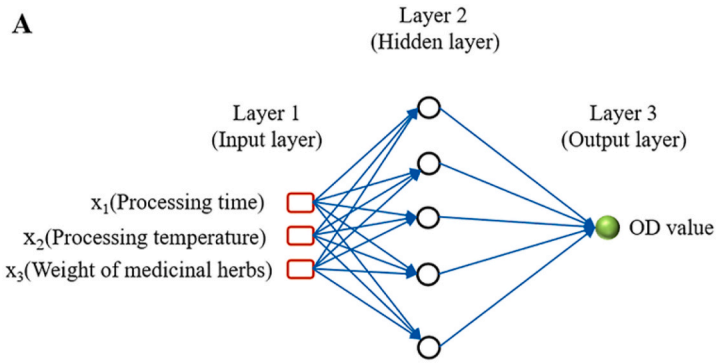


Fig. 1. Response surface for the combined effect of processing time and processing temperature (A, D); response surface for the combined effect of processing time and weight of herbs (B, E); response surface for the combined effect of processing temperature and weight of herbs (C, F).



(caption on next page)

Fig. 2. ANN modelling and training. Optimal architecture of developed ANN model (A); ANN training performance of OD (B); regression of experimental and predicted values in ANN model of OD (C).

time, 180 °C of processing temperature, and the herbs/machine volume 70 g/5 L were selected as the best single factor conditions. Additionally, the response surface methodology was further optimized.

3.1.3. RSM experiment

The one-factor experiment, processing temperature, time, and herbs/machine volume significantly influenced the response value. The RSM model was performed with Design-Expert software (version 8.0.6, Stat-Ease, Inc., Minneapolis, MN, USA). To obtain the optimized processing technology based on OD (TFC, TTC, and AC), a three-level BBD was used. Based on the results of the one-factor experiments, the RSM was developed, and 17 run samples were obtained (Table 1).

RSM must evaluate the fitness of the experimental values of the model to achieve better precision in the prediction process [20]. The ANOVA results were shown in Table S4. The models had a high F value (40.77) and a low p value ($p < 0.0001$), indicating the model's significance. R^2 of the experimental values was higher, indicating that the model is best fitted. The higher value (close to 1) of R^2 represents a better fit for the responses with second-order polynomial equations [9]. A more appropriate statistical model can be obtained by the low difference between R^2 (0.9813) and adjusted R^2 (0.9572). The R^2 values of all responses fall within the acceptable range ($R^2 \geq 0.80$), revealing the effects of variables on the examined parameters with good reliability in this study [9]. Furthermore, the lack of a fit test, which determines the adequacy of the selected model to describe variations in the experimental data around the fitted model, revealed a significantly small F value = 3.75, and an insignificant p value = 0.1171. These values indicated that the lack of fit was not significant relative to the pure error, inferring that the model was appropriate indeed. A model with ill-fitting data might exhibit a significant lack of fit ($p > 0.05$). Therefore proceeding with the optimization of the fitted response could yield poor or misleading results. The results suggested that the model could make adequate predictions within the range of the variables employed [21].

Multiple regression equations were generated to relate the response variable to the coding level of the independent variable. Using least-squares to predict the OD of processed products, a quadratic polynomial model determined the multiple regression coefficients. The data for the coding levels of the independent and response variables were analyzed to obtain the regression equations as follows:

$$Y = 0.93 + 0.060A - 0.018B + 0.065C - 0.11AB + 0.076AC + 0.037BC - 0.34A^2 - 0.46B^2 - 0.38C^2 \quad (4)$$

Three-dimensional (3-D) response surface plots were illustrated by showing the influences of processing conditions on the response variables to obtain the clarified view. The contour plot reflected the important influence of various interaction factors on the overall evaluation of SHC OD. The steeper the curve, the greater the comprehensive processing conditions for SHC's evaluation of OD. The 3-D response surface curves (A-C) and contour maps (D-F) of the interaction of various factors are shown in Fig. 1. The optimum processing process for SHC was a processing time of 10 min, processing temperature of 178 °C, and herbs/machine volume of 77 g based on the RSM data analysis. The predicted OD value was 0.9412 under these conditions. Compared to the predicted value, the OD value obtained through experimental validation was 0.9187 ($n = 3$), with an RSD of <3%.

3.1.4. ANN model

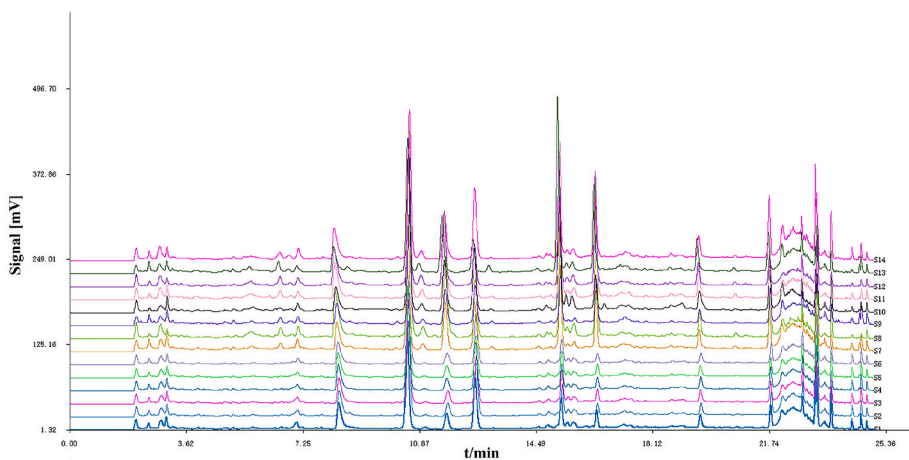
In the literature, ANN model is thought to be better and more sophisticated compared to RSM model. ANN is developing as an alternative to the RSM system of the complex nonlinear multivariate model. It is more precise compared to RSM in having a fitting experimental response, prediction, and model of herb processing [22]. The experimental values were subjected to the ANN model for further verification (Table 1). ANN is generated based on experimental BBD matrix data, comparing three layers (X_1 , X_2 , X_3), a hidden layer, and an output layer (Y). Using the hit and trial method, the number of neurons in the hidden layer was optimized by estimating the error between the network training and testing. The least training and testing errors were obtained as measures of the network performance of optimized topology during the process of development. The minimum error between testing and training was calculated for the optimum topology and the epochs were restricted to the lowest numbers to avoid model overfitting in the current experiment, paralleling the outcomes of other reports [23,24]. In the ANN model, a three-layer network containing two layers and five neurons was constructed and the data was trained (70%) and tested (30%) using the Levenberg-Marquardt algorithm (Fig. 2A). The

Table 2
Predictive capacity comparison of RSM and ANN models for a response variable.

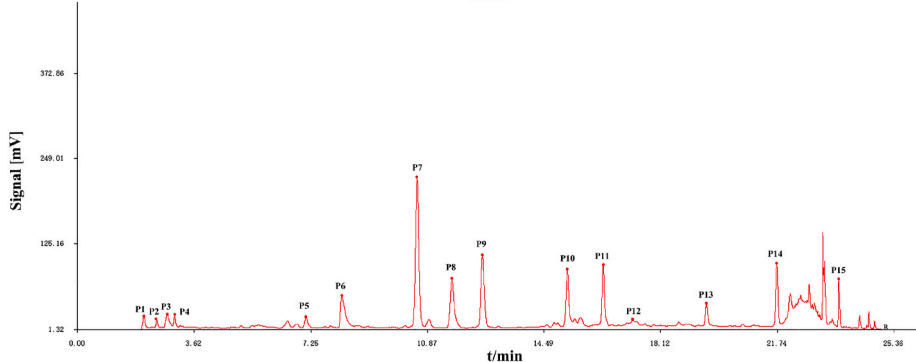
Parameters	OD	
	RSM	ANN
R^2 (%)	99.06	99.12
RMSE	0.87	0.05
MAE	0.046	0.036
SEP (%)	5.41	5.26

Abbreviation of each terms was; R^2 : correlation coefficients, RMSE: root mean square error, MAE: average absolute error, SEP: standard error of prediction.

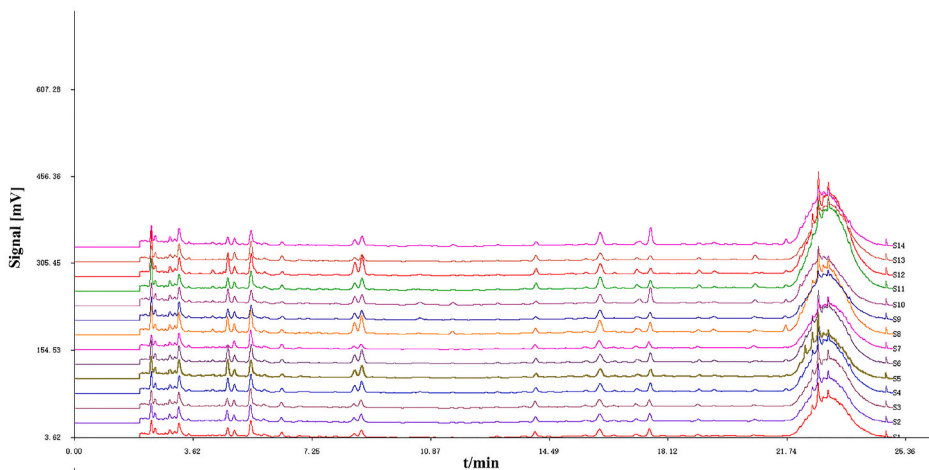
A1



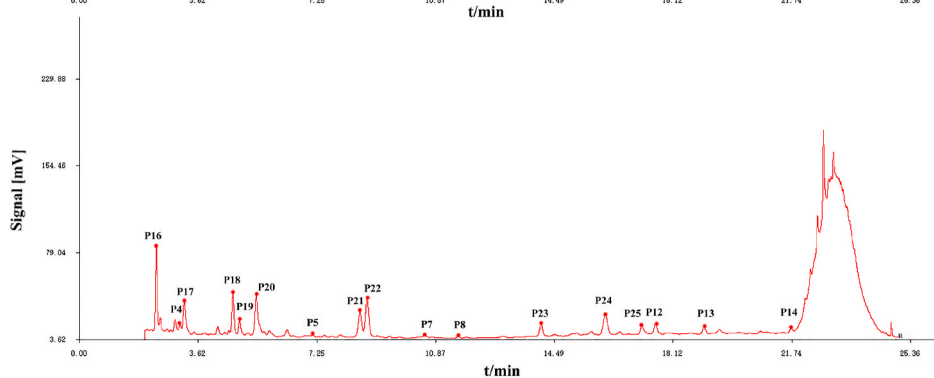
A2



B1



B2



(caption on next page)

Fig. 3. UPLC fingerprints (A1, B1) and reference fingerprint (A2, B2) of 14 batches (S1–S14) SH and 14 batches (S1–S14) SHC.

entire dataset of 17 runs was divided into three sets as follows: training had eleven points, validation had three points, and testing had three points. The Levenberg-Marquardt algorithm for network training resulted in the best validation performance for the OD, the dependent variable (Fig. 2B). The MSE of the OD dropped rapidly in the beginning, reaching the best validation performance of 0.0024872 at epoch five, where the OD shows the MSE. Training stops at this stage, weights and biases are applied to the process to generate the ANN model [25]. A good level of predictive power was obtained for the predicted data for OD and all regression correlation coefficient (R) values associated with OD were ≥ 0.98 for training, validation, testing, and the entire model (Fig. 2C). The predicted value obtained after training the ANN model is shown in Table 1. To overcome the uncertainties and limitations of the ANN model, numerous approaches have been applied [26,27]. For instance, the Bayesian statistical approach, step-wise regression, and ensemble method coupled with the ANN approach, have been reported in studies [28].

3.1.5. Comparison between RSM and ANN models

The comparative error analysis between the RSM and ANN models is shown in Table 2. Correlation coefficients (R^2), the root mean square error (RMSE), mean absolute error (MAE), and standard error of prediction (SEP) were calculated. Based on various parameters, such as R^2 , RMSE, and SEP, the predictive competence of the RSM and ANN models was determined and compared [29]. The R^2 reflects the reliability of the model, and the model is better the closer its value is to one. The RMSE values indicate the absolute fit of the model. The MAE accurately reflects the error between the predicted and the experiment values. The smaller the MAE, the closer the predicted value is to the true value, and the more accurate the prediction is. The RMSE, MAE, and SEP values should be lower for a better model, whereas the R^2 should be higher. The ANN performed better in terms of estimation and predictive capabilities, with a higher R^2 and lower MAE, RMSE, and SEP values compared to RSM.

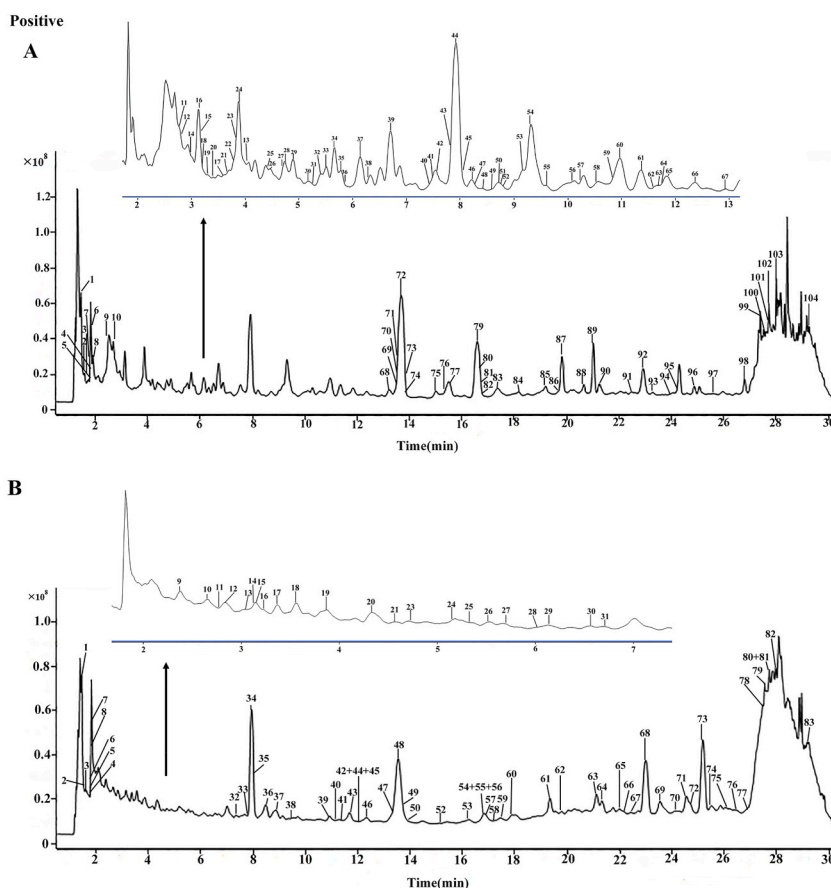


Fig. 4. The typical total ion chromatograms of SH (A) and SHC (B) samples in positive ion mode.

Table 3
Qualitative analysis and relative content of nonvolatile compounds in SH and SHC.

Peak no.	Retention time (min)		(M + H) ⁺	Formula	Error (ppm)		Fragment ions (m/z)	Identification
	SH	SHC			SH	SHC		
1	2	1.457	294.1547	C ₁₂ H ₂₃ NO ₇	3.94	1.7	294.1400, 248.1490, 258.1344, 276.1438, 215.1070, 202.0872, 171.9802	1-deoxy-1-L-leucine-d-fructuc acid
2	4	1.64	284.0989	C ₁₀ H ₁₃ N ₅ O ₅	1.96	3.73	284.0994	2-Hydroxyadenosine
3	3	1.664	268.1040	C ₁₀ H ₁₃ N ₅ O ₄	3.91	3.01	268.1051, 137.0461, 136.0616, 138.0510, 139.0468, 119.0350, 110.0353	Adenosine
4	5	1.698	136.0618	C ₅ H ₅ N ₅	-2.05	-1.76	136.0619, 137.0461, 138.0512, 119.0354, 120.0197, 94.0403, 67.0291	Adenine
5	6	1.707	294.1547 (M + NH ₄) ⁺	C ₁₂ H ₂₀ O ₇	2.11	0.76	294.1557, 139.0503, 230.1400, 258.1344, 159.0668	Triethyl citrate
6	1	1.84	132.1019	C ₆ H ₁₃ NO ₂	4.25	1.79	132.1019	L-leucine
7	7	1.853	150.0913	C ₉ H ₁₁ NO	1.63	3.84	150.0913	(+)-1-phenyl-2-imino-1-propanol
8	8	1.94	166.0863	C ₉ H ₁₁ NO ₂	3.9	1.6	166.0861, 149.0951, 123.0445, 120.0809, 109.0647, 91.0544, 81.0700	L- phenylalanine
9	-	2.605	276.2084	C ₁₈ H ₂₇ O ₂	0.33	-	276.2074, 157.1338, 259.1810, 233.1662, 202.1228, 188.1075	-
10	-	2.721	265.1547 (M + NH ₄) ⁺	C ₁₄ H ₁₇ NO ₃	2.84	-	265.1554	Fagaramide
11	11	2.788	139.0390	C ₇ H ₆ O ₃	2.88	1.64	139.0392, 121.0285, 122.0319, 93.0337, 94.0373, 66.0415, 65.0388	P-Hydroxybenzoic acid
12	12	2.804	148.1121	C ₁₀ H ₁₃ N	2.65	1.62	148.1121	N,N-Dimethyl-4-vinylaniline
13	10	2.854	225.0757	C ₁₁ H ₁₂ O ₅	2.83	-0.44	225.1490, 155.0865, 149.0950, 145.1000, 125.0602, 119.0858	Sinapic acid
14	13	3.021	190.0499	C ₁₀ H ₇ NO ₃	3.02	2.56	190.0506	2-Hydroxyquinoline-4-carboxylic acid
15	14	3.12	344.1353	C ₁₆ H ₁₇ N ₅ O ₄	0.41	-0.15	344.1357, 165.0549, 147.0445, 127.0393, 109.0287, 97.0284, 85.0285	N6-phenyladenosine
16	20	3.137	165.0546	C ₉ H ₈ O ₃	3.84	2.89	165.0551, 149.0235, 137.0598, 119.0491, 109.0650, 96.0442, 91.0544	p-Coumaric acid
17	15	3.137	147.0441	C ₉ H ₆ O ₂	3.37	5	147.0445	Coumarin
18	16	3.237	127.0390	C ₆ H ₆ O ₃	3.64	3.24	127.0394, 109.0286, 97.0284, 81.0336, 69.0337, 53.0390	Phloroglucinol
19	-	3.32	291.0863	C ₁₅ H ₁₄ O ₆	3.07	-	291.0863, 95.0852, 179.0329, 147.0412, 123.0444, 111.0443, 83.0496	Catechin
-	17	3.398	261.0982	C ₁₂ H ₁₂ N ₄ O ₃	-	0.73	261.0979, 81.0336, 237.9926, 218.0816, 196.9658, 113.0596	-
20	-	3.553	301.1071	C ₁₇ H ₁₆ O ₅	4.94	-	301.1071	4'-Hydroxy-5,7-dimethoxyflavanone
-	18	3.565	167.0703	C ₉ H ₁₀ O ₃	-	3.6	167.0706, 121.0648, 109.0650, 91.0544, 81.0700, 79.0545, 77.0389	Ethyl 4-hydroxybenzoate
21	9	3.586	195.0652	C ₁₀ H ₁₀ O ₄	3.72	2.54	195.0656, 125.0597, 123.0804, 121.0649, 131.0489, 133.0648, 135.0443	Isoferulic acid
22	19	3.752	137.0597	C ₈ H ₈ O ₂	0.08	1.67	137.0597, 122.0366, 94.0415, 66.0466, 51.0231	Methyl benzoate
23	-	3.869	389.1806	C ₁₈ H ₂₈ O ₉	2.75	-	389.1806	Jasmonic acid-5'-O-glucoside
24	-	3.885	389.1806	C ₁₈ H ₂₈ O ₉	2.34	-	389.1806	Hydroxyjasmonic acid hexose
25	-	4.418	329.1595	C ₁₆ H ₂₄ O ₇	2.65	-	329.1605, 149.0960, 167.1067, 121.1014, 93.0699, 75.0439, 198.1133, 222.1489, 276.8796, 317.0260	Rhododendrol-4'-O-β-D-glucopyranoside
26	-	4.534	137.1073	C ₈ H ₁₂ N ₂	1.38	-	137.1075, 60.9871, 61.0035, 66.0467, 70.9427, 103.0129, 107.0726	2,3,5,6-Tetramethylpyrazine

(continued on next page)

Table 3 (continued)

Peak no.		Retention time (min)	(M + H) ⁺	Formula	Error (ppm)		Fragment ions (m/z)	Identification
SH	SHC				SH	SHC		
–	21	4.569	264.1091	C ₁₁ H ₁₃ N ₅ O ₃	–	-1.61	264.1088, 247.0979, 237.9927, 223.9771, 196.9658	–
27	22	4.634	179.035 (M – H) ⁺	C ₉ H ₈ O ₄	0.32	0.35	179.0355, 135.0451, 134.0373, 136.0483	Caffeic acid
–	23	4.735	227.0914	C ₁₁ H ₁₄ O ₅	–	2.76	227.0921, 181.0499, 140.0469, 73.0286, 82.0416, 77.0388, 79.0554	–
28	–	4.767	167.1067	C ₁₀ H ₁₄ O ₂	2.96	–	167.1070, 91.0545, 92.0577, 93.0701, 94.0734, 149.0962, 131.0855	Nepetalactone
29	–	4.883	169.0495	C ₈ H ₈ O ₄	2.41	–	169.0500, 137.0234, 138.0266, 109.0286, 111.0805, 81.0338, 79.0546	–
30	24	5.167	155.0339	C ₇ H ₆ O ₄	3.95	1.92	155.0339	Protocatechuic acid
31	–	5.183	565.1552	C ₂₆ H ₂₈ O ₁₄	3.1	–	565.1552	Schaftoside
–	25	5.234	169.0495	C ₈ H ₈ O ₄	–	2.93	169.0497, 137.0234, 138.0266, 109.0286, 111.0805, 81.0338, 79.0546	–
32	–	5.366	153.0546	C ₈ H ₈ O ₃	3.23	–	153.0551, 121.0283, 136.0999, 125.0784, 111.0439, 109.0642, 108.0810, 107.0858, 96.0211, 95.0857, 93.9735, 91.0545, 79.0547	M-anisic-acid
–	26	5.533	157.0859	C ₈ H ₁₂ O ₃	–	3.71	157.0864, 111.0805, 93.0699, 67.0543, 57.0339, 77.0387, 65.0387, 91.0539, 115.0534, 130.0635, 143.0716	–
33	39	5.549	595.1657	C ₂₇ H ₃₀ O ₁₅	2.73	–	595.1657, 287.0556, 449.1093, 147.0655, 129.0544, 85.0283, 71.0495	Kaempferol-3-glucose-7-rhamnoside
34	30	5.615	355.1024	C ₁₆ H ₁₈ O ₉	3.93	3.58	355.1024	Neochlorogenic acid
–	27	5.733	313.1408	C ₁₅ H ₁₆ N ₆ O ₂	–	-0.39	313.1405, 127.0395, 81.0335, 97.0286, 107.0482, 111.0433, 134.0604, 167.0335	–
35	–	5.781	314.1598	C ₁₅ H ₂₃ NO ₆	3.98	–	314.1608	Sesbanimidec
36	28	5.971	227.1278	C ₁₂ H ₁₈ O ₄	2.81	2.88	227.1281, 212.1162, 185.0896, 168.0809, 149.0966, 131.0854, 105.0705, 91.0542, 79.0388, 67.0546	Jasmonic acid
37	29	6.164	227.1278	C ₁₂ H ₁₈ O ₄	0.49	2.07	227.1279, 210.1207, 209.1170, 192.1101, 191.1064, 168.1101, 167.1064, 137.0387, 131.0851	Fatty acid oxidation
38	–	6.23	241.1071	C ₁₂ H ₁₆ O ₅	3.08	–	241.1071	–
–	31	6.766	169.1223	C ₁₀ H ₁₆ O ₂	–	-2.53	169.1223, 93.0702, 105.0699, 109.1015, 123.1171, 133.1009, 151.1116, 156.0922	–
39	–	6.817	169.1223	C ₁₀ H ₁₆ O ₂	3.1	–	169.1225, 93.0702, 81.0701, 105.0699, 109.1015, 123.1171, 133.1009, 151.1116, 156.0922	–
40	–	7.378	369.1180	C ₁₇ H ₂₀ O ₉	3.54	–	369.118	Feruloylquinic
41	32	7.478	185.1172	C ₁₀ H ₁₆ O ₃	3.14	3.41	185.1172	–
42	–	7.567	374.1446					
(M + NH ₄) ⁺	C ₁₆ H ₂₀ O ₉	3.85	–	374.1459, 91.0545, 127.0392, 105.0183				Gentiopicroside
43	33	7.956	303.0499	C ₁₅ H ₁₀ O ₇	3.69	2.88	303.0511, 285.0399, 257.0446, 229.0498, 153.0180, 137.0231	Quercetin
44	34	7.961	611.1607	C ₂₇ H ₃₀ O ₁₆	0	0	611.1639, 465.1039, 303.0513, 304.0544, 305.0565, 147.0654, 129.0549, 97.0284, 86.0321	Rutinum
45	35	8.027	465.1028	C ₂₁ H ₂₀ O ₁₂	3.38	3.72	465.1028	Isoquercitrin
46	–	8.226	595.1657	C ₂₇ H ₃₀ O ₁₅	2.94	–	595.1684, 287.0557, 449.1087, 417.1569, 341.1380, 129.0543	Luteolin 7-O-rutinoside
47	–	8.226	595.1657	C ₂₇ H ₃₀ O ₁₅	2.73	–	595.1657	Kaempferol-7-neohesperidoside
48	–	8.261	433.1129	C ₂₁ H ₂₀ O ₁₀	2.21	–	433.1142, 271.0606, 153.0181, 119.0181, 85.0284	Vitexin

(continued on next page)

Table 3 (continued)

Peak no.		Retention time (min)	(M + H) ⁺	Formula	Error (ppm)		Fragment ions (m/z)	Identification
SH	SHC				SH	SHC		
49	–	8.273	757.1974	C ₃₆ H ₃₆ O ₁₈	0.71	–	757.1974	Shisolamin
–	36	8.46	211.0978	C ₁₂ H ₁₀ N ₄	–	-0.91	211.0973, 137.0599, 122.0365, 107.0490, 94.0415, 77.0388	–
50	–	8.702	289.0707	C ₁₅ H ₁₂ O ₆	3.4	–	289.0714, 153.0813, 163.0391, 145.0274, 95.0863, 81.0698, 67.0177	Eriodictyol
51	–	8.758	451.1235	C ₂₁ H ₂₂ O ₁₁	2.5	–	451.1235	–
52	–	8.858	307.0812	C ₁₅ H ₁₄ O ₇	4.79	–	307.0812	(–)-gallicocatechin
–	37	8.86	281.1033	C ₁₅ H ₁₂ N ₄ O ₂	–	-0.13	281.1029, 263.0921, 221.0812, 187.0757, 159.0807, 127.0393	–
53	–	9.257	199.0601	C ₉ H ₁₀ O ₅	2.75	–	199.0607	Syringate
54	–	9.306	449.1078	C ₂₁ H ₂₀ O ₁₁	0.86	–	449.1086, 450.1122, 287.0556, 153.0179	Luteoloside
–	38	9.525	197.0808	C ₁₀ H ₁₂ O ₄	–	3.39	197.0813, 140.0475, 196.9657, 125.0238, 97.0285, 77.0390, 56.9425	Acetosyringone
55	–	9.623	595.1657	C ₂₇ H ₃₀ O ₁₅	2.73	–	595.1657	Kaempferol-3-rutinoside
56	–	10.139	137.1325	C ₁₀ H ₁₆	1.37	–	137.1325	γ-Terpinene
57	–	10.255	331.0812	C ₁₇ H ₁₄ O ₇	3.1	–	331.0811, 315.0496, 316.0539, 317.0562, 299.0543, 298.0466, 296.8841, 151.1116, 131.0487	Tricin
58	–	10.555	123.0441	C ₇ H ₆ O ₂	1.58	–	123.0794, 77.0386, 79.0543, 105.0339, 108.0678	Benzoic acid
59	40	10.804	595.1657	C ₂₇ H ₃₀ O ₁₅	2.73	3.13	595.1657	Kaempferol-7-rutinoside
60	–	10.986	348.2030	C ₁₇ H ₂₅ N ₅ O ₃	1.21	–	348.2031, 169.1226, 151.1119, 133.1010, 145.0496, 109.1017, 105.0699, 93.0701	–
–	41	11.005	348.2030	C ₁₇ H ₂₅ N ₅ O ₃	–	-0.21	348.2030, 169.1226, 151.1119, 133.1010, 145.0496, 109.1017, 105.0699, 93.0701	–
61	–	11.404	417.1769	C ₂₀ H ₂₄ N ₄ O ₆	0.43	–	417.1769, 207.0631, 181.0491, 169.1226, 151.1118, 145.0508	–
62	–	11.552	579.1708	C ₂₇ H ₃₀ O ₁₄	2.95	–	579.1734, 271.0607, 433.1138, 417.1177, 129.0544, 105.0176	Apeginin-o-rhamnosylhexoside
63	44	11.627	317.0656	C ₁₆ H ₁₂ O ₇	2.93	3.55	317.0656	Eupafolin
64	42	11.652	479.1184	C ₂₂ H ₂₂ O ₁₂	3.12	2.89	479.1198, 317.0664, 318.0707, 267.0920, 181.0496, 199.0594	Pollenitin B
–	43	11.67	330.1561	C ₁₆ H ₁₉ N ₅ O ₃	–	-0.62	330.1562, 187.0607, 127.0392, 109.0287, 97.0286, 91.0545, 85.0285	–
65	–	11.82	598.2508	C ₂₉ H ₃₅ N ₅ O ₉	1.43	–	598.2515, 401.1606, 383.1499, 371.1505, 351.1229, 330.1104, 265.1078, 247.0964, 235.0970, 217.0859, 205.0864	–
–	45	11.87	598.2508	C ₂₉ H ₃₅ N ₅ O ₉	–	-0.13	598.2508, 401.1606, 383.1499, 371.1505, 351.1229, 330.1104, 265.1078, 247.0964, 235.0970, 217.0859, 205.0864, 180.0871, 167.0700, 145.0498, 190.0625, 173.0599, 81.0337	–
–	46	12.319	251.0914	C ₁₃ H ₁₄ O ₅	–	2.52	251.0923, 233.0820, 223.9769, 177.0548, 149.0602, 131.0753	–
66	–	12.371	366.1772	C ₁₆ H ₂₃ N ₅ O ₅	-0.58	–	366.1770, 295.1180, 231.0503, 209.1171, 189.0398, 171.1391, 159.0291, 145.0496, 127.0392, 105.0183, 97.0283	–
67	–	13.116	273.0757	C ₁₅ H ₁₂ O ₅	0.25	–	273.0757	Naringenin
68	–	13.204	461.1819	C ₂₅ H ₂₄ N ₄ O ₅	0.55	–	461.1821, 425.1608, 317.1385, 299.1285, 271.0972, 175.0756, 151.0752, 137.0596, 99.0439, 83.0497, 81.0338, 69.0334, 53.0388	–
69	–	13.493	433.1129	C ₂₁ H ₂₀ O ₁₀	3.67	–	433.1129, 271.0608, 153.0182, 119.0489	Apigenin-7-O-glucoside
70	48	13.515	209.0808	C ₁₁ H ₁₂ O ₄	2.55	4.35	209.0814, 178.0260, 191.0706, 163.0396, 147.0443, 133.0285, 91.0545, 89.0385	3,4-dimethoxycinnamic acid

(continued on next page)

Table 3 (continued)

Peak no.		Retention time (min)	(M + H) ⁺	Formula	Error (ppm)		Fragment ions (m/z)	Identification
SH	SHC				SH	SHC		
71	47	13.565	149.0597	C ₉ H ₈ O ₂	3.01	3.74	149.0602, 134.0358, 121.0647, 106.0412, 91.0546, 77.0388, 65.0391	Cinnamic acid
72	49	13.733	611.1970	C ₂₈ H ₃₄ O ₁₅	1.53	1.5	611.1978, 449.1448, 303.0866, 345.0970	Hesperidin
73	50	13.743	303.0863	C ₁₆ H ₁₄ O ₆	3.68	2.37	303.0868, 285.0759, 219.0647, 201.0549, 177.0546, 153.0183, 145.0284	Hesperetin
74	–	13.947	447.0922	C ₂₁ H ₁₈ O ₁₁	2.73	–	447.0922	Apigenin-7-o-glucuronide
75	–	15.028	535.1082	C ₂₄ H ₂₂ O ₁₄	2.63	–	535.1096, 449.1091, 287.0558, 288.0588, 289.0609	Flavone base+4O,malonylhex
76	52	15.411	163.0390	C ₉ H ₆ O ₃	3.75	3.56	163.0395, 107.0491, 77.0390, 79.0545, 63.0231, 163.0393, 135.0441	Umbelliferone
77	–	15.456	846.4879	C ₄₉ H ₇₀ ClN ₄ O ₄ S	0	–	846.4873, 469.3324, 451.3220, 487.3429, 342.1402, 325.1138, 441.3372, 423.3267, 405.3162, 205.1589	–
78	51	15.599	359.0772	C ₁₈ H ₁₆ O ₈	0.39	0.32	359.0778, 197.0457, 161.0246, 135.0450	Rosmarinic acid
79	54	16.476	463.0871	C ₂₁ H ₁₈ O ₁₂	0.47	3.87	463.087, 287.0555, 288.0585, 289.0612, 153.0177	Kaempferol-3-glucuronide
80	55	16.476	463.0871	C ₂₁ H ₁₈ O ₁₂	0.47	3.87	463.0889, 287.0560, 463.0884, 288.0593, 289.0612, 153.0182	Scutellarin
81	56	16.476	463.0871	C ₂₁ H ₁₈ O ₁₂	0.47	3.87	463.0884, 287.0560, 288.0593, 289.0612, 153.0182	Luteolin-7-O-glucuronide
–	57	16.859	319.119	C ₁₈ H ₁₄ N ₄ O ₂	–	0	319.1189	–
82	53	17.024	435.1650	C ₂₂ H ₂₆ O ₉	2.26	3.13	435.1663, 181.0496, 167.0704, 233.0802, 107.0501, 88.0218	Ciwujiatone
–	58	17.042	249.1121	C ₁₄ H ₁₆ O ₄	–	3.13	249.1129, 223.9766, 196.9661, 115.0541, 91.0545	–
83	59	17.325	151.1117	C ₁₀ H ₁₄ O	1.69	2.16	151.1118, 81.0701, 109.0650, 123.1170, 79.0544	(–)-VERBENONE
–	60	17.907	219.1016	C ₁₃ H ₁₄ O ₃	–	2.52	219.1019, 201.0905, 189.0911, 174.0671, 129.0701, 119.0489, 91.0544, 58.0654, 128.0620, 115.0542	–
84	–	18.158	846.4879	C ₄₉ H ₇₀ ClN ₄ O ₄ S	0	–	846.4873, 469.3324, 451.3220, 487.3429, 342.1402, 325.1138, 441.3372, 423.3267, 405.3162, 205.1589	–
85	–	19.175	434.2034	C ₂₀ H ₂₇ N ₅ O ₆	0.95	–	434.2033, 231.0501, 169.1224, 151.1118, 145.0499, 127.0392, 109.0286	–
–	61	19.321	401.1622	C ₂₅ H ₂₂ NO ₄	–	-1.61	401.1611, 383.1499, 368.1262, 167.0702, 353.1027, 264.0785, 247.0755, 219.0806, 156.0570, 107.0490, 79.0545	–
86	–	19.613	155.1430	C ₁₀ H ₁₈ O	1.97	–	155.143	Menthone
–	62	19.819	371.1503	C ₂₂ H ₁₈ N ₄ O ₂	–	-0.39	371.1501, 353.1391, 217.0865, 167.0702, 137.0595, 107.0493, 123.0445, 234.0673	–
87	–	19.875	736.1895	C ₂₈ H ₄₆ Cl ₃ N ₄ O ₈ S ₂	0	–	736.1898, 559.0880, 521.1093, 519.1156, 493.1134, 411.0722, 365.0653, 341.0667, 323.0558, 295.0607	–
88	–	20.676	714.2994	C ₃₆ H ₄₅ N ₂ O ₁₃	-0.73	–	714.2991, 517.2078, 505.2084, 487.1975, 469.1872, 361.1658, 343.1549, 315.1234, 207.1020, 189.0910, 151.0755, 127.0392	–
89	–	21.009	684.2889	C ₃₅ H ₄₃ N ₂ O ₁₂	0.09	–	684.2891, 487.1972, 475.1984, 457.1871, 439.1763, 351.1451, 331.1549, 313.1441, 287.1281, 189.0910, 151.0755, 127.0392	–
–	63	21.133	349.1295	C ₁₉ H ₁₆ N ₄ O ₃	–	1.19	349.1300, 195.0654, 181.0499, 167.0705, 151.0756, 123.0441, 107.0491	–

(continued on next page)

Table 3 (continued)

Peak no.		Retention time (min)	(M + H) ⁺	Formula	Error (ppm)		Fragment ions (m/z)	Identification
SH	SHC				SH	SHC		
-	64	21.316	361.1295	C ₂₀ H ₁₆ N ₄ O ₃	-	1.04	361.1293, 343.1183, 329.1024, 301.1076, 207.0656, 179.0704, 167.0704, 147.0442, 285.0765, 119.0491, 91.0545	-
90	-	21.343	430.1721	C ₂₀ H ₂₃ N ₅ O ₆	1.19	-	430.1723, 273.1130, 231.0503, 159.0291, 145.0495, 127.0392, 105.0182, 85.0285, 181.0491, 109.0286, 97.0285, 69.0339	-
-	65	22.015	289.1084	C ₁₇ H ₁₂ N ₄ O	-	-1.1	289.1078, 271.0974, 165.0547, 151.0391, 137.0597, 123.0440, 108.0204, 94.0413	-
-	66	22.115	291.0863	C ₁₅ H ₁₄ O ₆	-	4.54	291.0863, 95.0852, 179.0329, 147.0412, 123.0444, 111.0443, 83.0496	L-epicatechin
91	-	22.429	329.1020	C ₁₈ H ₁₆ O ₆	3.44	-	329.102	Salvigenin
-	67	22.464	331.119	C ₁₉ H ₁₄ N ₄ O ₂	-	-0.37	331.1187, 313.1079, 177.0549, 154.0627, 131.0487, 181.0643, 165.0701, 139.0390	-
92	68	22.98	287.0550	C ₁₅ H ₁₀ O ₆	0.73	3.34	287.0554, 153.0181, 161.0246, 135.0441	Luteolin
93	-	23.344	830.4928	C ₃₀ H ₆₅ N ₁₄ O ₁₃	-0.4	-	830.4924, 831.4953, 796.1494, 772.9076, 755.4928, 407.3321, 425.3422, 443.3537, 453.3379, 471.3478, 489.3593, 342.1398	-
-	69	23.545	371.1503	C ₂₂ H ₁₈ N ₄ O ₂	-	0.56	371.1501, 353.1395, 321.1129, 309.1127, 300.0997, 293.1182, 247.0971, 217.0861, 167.0704, 137.0596, 285.0764, 239.0707	-
94	-	24.192	285.0757	C ₁₆ H ₁₂ O ₅	3.14	-	285.0767, 286.0801, 287.0555	Physcion
95	70	24.261	301.0707	C ₁₆ H ₁₂ O ₆	3.1	3.49	301.0719, 168.0054, 286.0478, 68.9972, 121.0284, 140.0103, 258.0530	Chrysoeriol
-	71	24.576	436.1993	C ₂₄ H ₂₁ N ₉	-	-0.67	436.1988, 401.1615, 217.0861, 205.0864, 190.0629, 167.0705, 315.0872, 173.0601, 167.0705, 145.0649, 107.0492, 81.0338	-
-	72	24.726	387.1465	C ₂₄ H ₂₀ NO ₄	-	-2.06	387.1452, 369.1351, 351.1238, 337.1081, 319.0968, 305.0816, 195.0655, 167.0702, 79.0543, 55.0181	-
96	-	25.09	830.4928	C ₃₀ H ₆₅ N ₁₄ O ₁₃	-0.4	-	830.4924, 831.4953, 796.1494, 772.9076, 755.4928, 407.3321, 425.3422, 443.3537, 453.3379	-
-	73	25.158	401.1622	C ₂₅ H ₂₂ NO ₄	-	-1.83	401.1611, 383.1510, 351.1238, 330.1105, 247.0966, 217.0863, 167.0705, 315.0871, 156.0572, 107.0489	-
97	-	25.44	331.0812	C ₁₇ H ₁₄ O ₇	3.1	-	331.0821, 316.0583, 288.0636, 151.0391	Cirsiliol
-	74	25.507	361.1295	C ₂₀ H ₁₆ N ₄ O ₃	-	-0.23	361.1293, 329.1029, 181.0497, 179.0704, 153.0558, 119.0491, 91.0543	-
-	75	26.289	477.1769	C ₂₅ H ₂₄ N ₄ O ₆	-	0.57	477.1773, 459.1656, 399.1450, 263.0916, 245.0814, 233.0815, 181.0499, 167.0705, 107.0491	-
-	76	26.505	417.1557	C ₂₃ H ₂₀ N ₄ O ₄	-	0.46	417.1559, 191.0708, 181.0498, 167.0703, 163.0754, 148.0520, 131.0491, 118.0413, 103.0544	-
98	-	26.746	734.1741	C ₂₈ H ₃₆ ClN ₅ O ₁₄ S	0	-	734.1740, 321.0402, 519.0934, 339.0503, 181.0496, 519.0936, 139.0388	-
-	77	26.871	734.1741	C ₂₈ H ₃₆ ClN ₅ O ₁₄ S	-	-0.27	734.1729, 321.0402, 519.0934, 339.0503, 181.0496, 519.0936, 139.0388	-
99	78	27.369	271.0601	C ₁₅ H ₁₀ O ₅	0.09	3.66	271.0601	Apigenin
100	79	27.542	301.0707	C ₁₆ H ₁₂ O ₆	-0.24	3.49	301.0705, 286.0473, 258.0522, 229.0473, 184.0523	Hispidulin

(continued on next page)

Table 3 (continued)

Peak no.		Retention time (min)	(M + H) ⁺	Formula	Error (ppm)		Fragment ions (m/z)	Identification
SH	SHC				SH	SHC		
101	80	27.649	301.0707	C ₁₆ H ₁₂ O ₆	-0.24	3.49	301.0705, 286.0473, 168.0052, 258.0522, 229.0473, 184.0523	Diosmetin
102	81	27.709	331.0812	C ₁₇ H ₁₄ O ₇	1.26	4.22	331.0811, 224.1276, 316.0577, 288.0641, 273.0391, 301.0350, 245.0450	Jaceosidin
103	82	28.001	345.0969	C ₁₈ H ₁₆ O ₇	5.12	5.31	345.0973, 329.0661, 314.0434, 301.0661, 284.0685, 169.0133, 69.0338	Eupatilin
104	83	29.165	153.1274	C ₁₀ H ₁₆ O	0.87	2.72	153.1264, 69.0697, 55.0542, 93.0701, 107.0853, 135.1166	Pulegone

Relative content (%) in the last two columns represents the mean ± SD (n = 14). - : unidentified.

3.2. The establishment of UPLC fingerprints

3.2.1. Method validation

The precision, repeatability, and stability of the established UPLC method were validated. The RSDs of intra and inter-day precision of the peak areas for the 15 common peaks were less than 2.87% and 2.91%, respectively (Table S5). The repeatability expressed as RSD was less than 2.84% and the stability was less than 2.67%. The method validation results indicated that the established UPLC method was suitable for analysing SH samples.

3.2.2. UPLC fingerprints and similarity analysis

The optimized processing method discussed was used to process 14 batches of SH collected from different regions and 14 batches of SHC were obtained. The SH and SHC samples were analyzed via UPLC. The Chinese Medicine Chromatographic Fingerprint Similarity Evaluation System (version 2004 A) was used to establish UPLC fingerprints (Fig. 3A1, 3B1 illustrate the fingerprints of the SH and SHC samples, while Fig. 3A2, 3B2 illustrate the reference fingerprints, respectively). As shown in Table S6, the similarity values for the UPLC fingerprints of the SH and SHC samples ranged from 0.900 to 0.990. This indicates the reproducibility of the processing technology established in this experiment.

3.3. UPLC-Q-TOF-MS data analysis

3.3.1. Identification of chemical compositions in SH and SHC samples via UPLC-Q-TOF-MS

The UPLC-Q-TOF-MS method was used to compare the overall nonvolatile chemical characteristics of SH and SHC in the positive (Fig. 4A) and negative (Fig. 4B) ion modes. Fig. 4 shows the total ion current chromatograms of SH and SHC in the positive ion mode (positive ion mode A: total ion current chromatogram of SH; B: total ion current chromatogram of SHC). The total ion current chromatograms of SH and SHC in negative ion mode are shown in Fig. S2 (negative ion mode A: total ion current chromatogram of SH; B: total ion current chromatogram of SHC). Qualitative and relative quantitative analysis of the collected raw data were performed using Agilent MassHunter workstation software (Qualitative analysis 10.0, Agilent Technologies, Santa Clara, CA, USA). By normalizing each extracted abundance with the abundance of the corresponding sample's internal standard, the relative content of the major compounds in each test sample was calculated. Compounds were resolved by searching databases and literature, such as ChemSpider, MassBank, and Agilent herbal library-v20-04-17, to tentatively identify them (Table 3).

3.3.2. Multivariate statistical analysis of chemical compositions in SH and SHC

Based on the results of UPLC-Q-TOF-MS analysis, a cluster analysis of 78 common components in 14 batches of SH and SHC was performed using SPSS software (version 22.0; IBM, Armonk, New York, United States). The dendrogram showed that SH and SHC samples could be divided into two groups (Fig. 5A). A PCA was performed, based on the LC-MS data of 78 common compounds, using SIMCA software (version 13.0, Umetrics, Umea, Sweden). The PCA ($R^2X = 0.768$, $Q^2 = 0.705$) and the scores plot showed that the 28 batches of samples were divided into two groups, aiding in further investigation of the quality variation and differentiation of SH and SHC samples (Fig. 5B). The result was the same as HCA. PCA is an unsupervised model, that considers all variables. However, OPLS-DA is a supervised model, which filtering system noise and extracting variable information. The OPLS-DA model is more efficient in its classification compared to the PCA model. To select the chemical markers responsible for such separation, the dataset was applied to OPLS-DA (Fig. 5C). The resulting values of R^2Y (cum) and Q^2 (cum) were 0.991 and 0.972, respectively. This indicated that the OPLS-DA model has good applicability and predictability. The OPLS-DA score plot showed a clear separation among the samples observed, where SH and SHC were located on both sides of the Y-axis, indicating that carbonation processing had a major effect on the composition of SH. To validate the model, a permutation test (n = 200) was done. The OPLS-DA model was found to be stable and reproducible ($R^2 = (0.0, 0.433)$, $Q^2 = (0.0, -0.453)$) (Fig. 5D). These results confirmed a significant difference between SH and SHC. Fifteen key constituents for discriminating SH and SHC were selected after screening by applying the thresholds "VIP > 1.10" and "p < 0.001". Detailed information concerning these chemical markers was summarized in Table S7, and their structures are shown in Fig. S3. The following six compounds were upregulated in SHC compared to those in SH: protocatechuic acid, caffeic acid, cinnamic

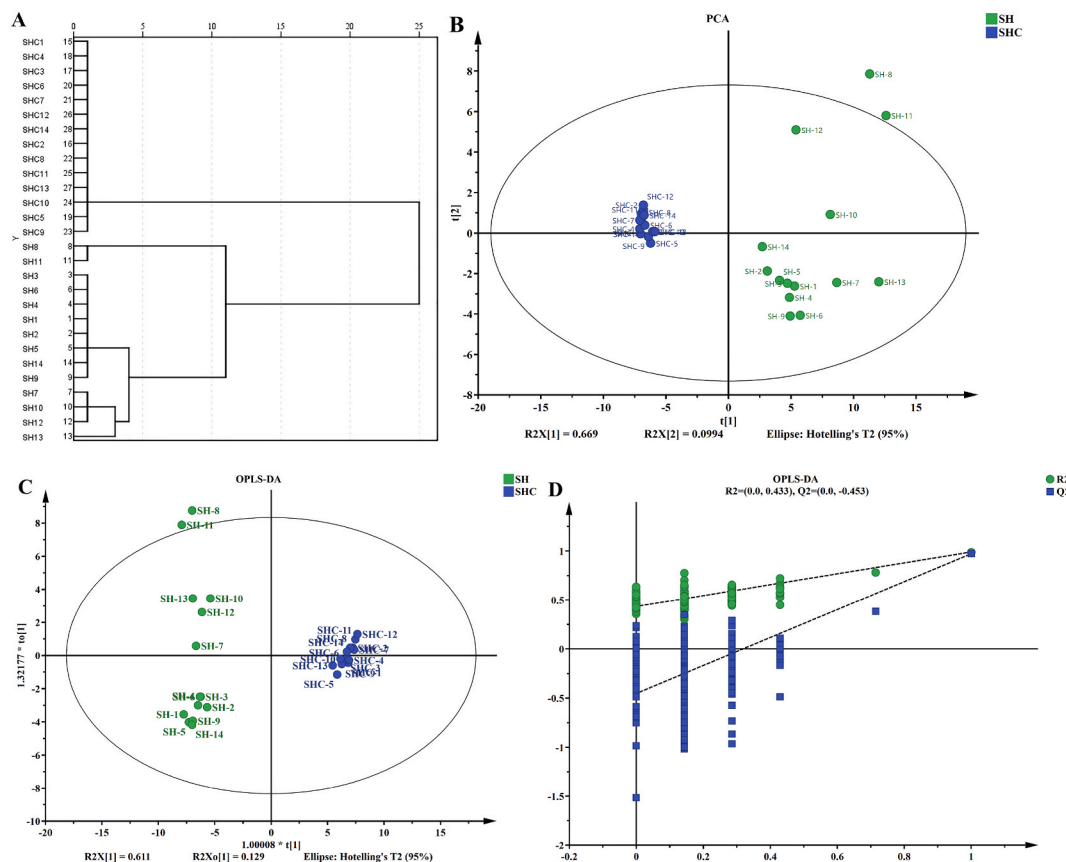


Fig. 5. Dendrogram of all samples analyzed (A). Unsupervised PCA score plot of SH and SHC samples (B). OPLS-DA score plot showing the discrimination the metabolome of SH and SHC. (R^2Y (cum) = 0.991; Q^2 (cum) = 0.972) (C). A presentation of chance permutation at 200 times used for the discrimination between the two groups. ($R^2 = (0.0, 0.433)$, $Q^2 = (0.0, -0.453)$) (D).

acid, isoferulic acid, lignocaine, and kaempferolic acid. In addition, nine compounds were downregulated in SH as follows: vitexin, rosmarinic acid, pulegone, hesperidin, luteoloside, scutellarin, hesperetin, nepetalactone, and naringenin (Fig. S4).

3.3.3. Possible mechanisms involved in the transformation of the nonvolatile compounds between SH and SHC

This study suggests that the decline of the relative content of luteoloside and rosmarinic acid may have caused the increase in luteolin and caffeic acid, respectively. The possible mechanisms involved in the conversion of these compounds were postulated in Fig. 6. It may be due to the breaking of the glycosidic bonds of luteoloside and hesperidin to produce the corresponding aglycone. Another postulation suggested the breaking of the ester bond of rosmarinic acid to produce caffeic acid during the stir-frying of SH into SHC to be responsible. The results are consistent with previous reports concerning glucoside being hydrolyzed to aglycone under various conditions, including the high temperature during stir-fry processing [30,31]. Additionally, luteoloside has been demonstrated to have significant anti-inflammatory, antiviral, anticancer, and analgesic effects [32]. Luteolin, which is a potential hemostatic candidate, may have similar effects [33]. Due to caffeic acid's promotion of hematopoiesis and hemostasis properties, it has been used in treating thrombocytopenia and leukopenia with various causes in China [34]. These findings support the traditional experience that SHC can be used in various bleeding disorders with astringent and hemostatic effects. A significant change was also noted in SH and SHC metabolites after carbonization. Whether or not these other altered substances are responsible for the changed pharmacological properties of raw SH after stir-fry processing needs to be determined by chemical and biological activity studies in the future.

4. Conclusion

To the best of our knowledge, this study was the first investigation to optimize the processing technology of SHC using two model approaches (RSM and ANN) and discover the chemical composition difference between SH and SHC via performing LC-MS/MS. The ANN model is acknowledged as a superior and sophisticated model, as it exhibited a higher R^2 and lower RMSE, MAE, and SEP compared to the RSM model. This suggests the models were accurate and reliable. The optimal process parameters for the SHC were as follows: 10 min of processing time, 178 °C for the processing temperature, and 77 g/5 L of the herbs/machine volume. In a chemical characterization of SH and SHC, 104 and 83 chemical compositions including organic acids and flavonoids were tentatively identified,

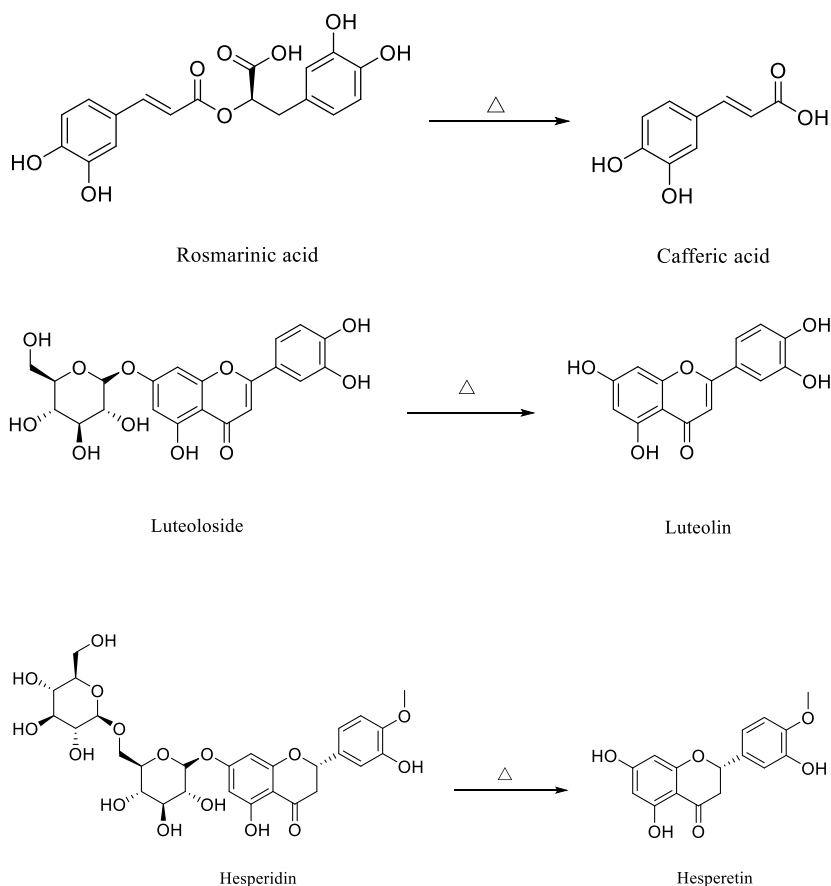


Fig. 6. Possible mechanisms involved in the transformation of some main nonvolatile components during the stir-fry processing of SHC.

respectively. In addition, PCA and OPLS-DA were used to find the potential chemical markers, and 15 compounds greatly differed between SH and SHC. This may explain why SH and SHC are used to treat different diseases in traditional Chinese medicine and modern pharmacology. Finally, the chemical transformation of SHC during stir-fry processing mechanisms was rationalized by deducing possible reactions involved in the transformation of these marker components. Although we have optimized the process technology using RSM and ANN models combined with multiple parameters, the resulting product still requires further activity validation for clinical application. This study provides a more reliable method for investigating quantifiable processing technology for medicinal herbs and new clues for the investigation of the induced chemical transformation of SHC via the stir-frying method.

Declarations

Author contribution statement

Xiaoying Ding; Huaiyou Wang: Conceived and designed the experiments; Performed the experiments; Analyzed and interpreted the data; Wrote the paper.

Hengyang Li; Tao Wang; Shenghui Hao; Wenjie Li; Chengyue Wang; Lei Wang; Yuguang Zheng: Analyzed and interpreted the data; Contributed reagents, materials, analysis tools or data.

Qi An; Long Guo; Dan Zhang: Conceived and designed the experiments; Contributed reagents, materials, analysis tools or data; Wrote the paper.

Funding statement

This work was supported by the Natural Science Foundation of Hebei Province (H2021423017, H2022418001), Key R&D plan of Hebei Province (22372503D), S&T Program of Hebei (223777127D, 226Z7714G), 333 Talent Project supported Project of Hebei Province (C20221005), the Scientific Research Programme of Hebei Provincial Administration of Traditional Chinese Medicine (2022101), the Innovation Team of Hebei Province Modern Agricultural Industry Technology System (HBCT2018060205), the Technology and Innovation Capabilities of University and High School Students of Hebei Province (2021H011607).

Data availability statement

Data included in article/supp. material/referenced in article.

Declaration of interest's statement

The authors declare no competing interests.

Appendix A. Supplementary data

Supplementary data related to this article can be found at <https://doi.org/10.1016/j.heliyon.2023.e13398>.

References

- [1] K. Ge, X.Y. Chen, Shi Yao Shen Shu, Pepole's medical publishing house, Beijing, 1956.
- [2] P. Wu, X.Y. Sun, F.J. Sun, Shen Nong Ben Cao Jing, People's Medical Publishing House, Beijing, 1984.
- [3] S.Z. Li, H.R. Liu, Ben Cao Gang Mu, People's Medical Publishing House, Beijing, 1982.
- [4] X. Liu, Z. Huang, J. Zhang, Y. Zhou, Y. Zhang, M. Wu, H. Cao, Comparisons of the anti-inflammatory, antiviral, and hemostatic activities and chemical profiles of raw and charred *Schizonepetae Spica*, *J. Ethnopharmacol.* 278 (2021), 114275.
- [5] D. Fung, C.B. Lau, *Schizonepeta tenuifolia*: chemistry, pharmacology, and clinical applications, *J. Clin. Pharmacol.* 42 (1) (2002) 30–36.
- [6] J. Liu, Y. Sun, L. Liu, C. Yu, The extraction process optimization and physicochemical properties of polysaccharides from the roots of *Euphorbia fisheriana*, *Int. J. Biol. Macromol.* 49 (3) (2011) 416–421.
- [7] S. Malairaj, S. Muthu, V.B. Gopal, P. Perumal, R. Ramasamy, Qualitative and quantitative determination of R-phycoerythrin from *Halymenia floresia* (Clemente) C. Agardh by polyacrylamide gel using electrophoretic elution technique, *J. Chromatogr. A* 1454 (2016) 120–126.
- [8] K.H. Musa, A. Abdullah, A. Al-Haiqi, Determination of DPPH free radical scavenging activity: application of artificial neural networks, *Food Chem.* 194 (2016) 705–711.
- [9] Q.Q. Yang, R.Y. Gan, D. Zhang, Y.Y. Ge, L.Z. Cheng, H. Corke, Optimization of kidney bean antioxidants using RSM & ANN and characterization of antioxidant profile by UPLC-QTOF-MS, *LWT-Food Sci. Technol.* 114 (2019), 108321.
- [10] H. Xue, J. Xu, J. Zhang, Y. Wei, X. Cai, J. Tan, Modeling, optimization, purification, and characterization of polysaccharides from *Lilium lancifolium* Thunb, *LWT-Food Sci. Technol.* 162 (2022), <https://doi.org/10.1016/j.lwt.2022.113491>.
- [11] T. Aung, S.-J. Kim, J.-B. Eun, A hybrid RSM-ANN-GA approach on optimisation of extraction conditions for bioactive component-rich laver (*Porphyra dentata*) extract, *Food Chem.* 366 (2022), <https://doi.org/10.1016/j.foodchem.2021.130689>.
- [12] K. Zheng, Y. Zhao, W. Li, Y. Li, T. Zhang, D. Chen, C. Hu, Optimization of processing technology of honey roasted Ligusticum Chuanxiong by box Behnken response surface method combined with artificial neural network, *J. Chin. Med. Mater.* 40 (9) (2017) 2055–2059.
- [13] X. Lizhai, Jiaozhu Furen Liangfang. Shanghai: Scitific and Health Publishes, 1958.
- [14] J.E. Li, S.T. Fan, Z.H. Qiu, C. Li, S.P. Nie, Total flavonoids content, antioxidant and antimicrobial activities of extracts from *Mosla chinensis* Maxim. cv. Jiangxiangru, *LWT-Food Sci. Technol.* 64 (2) (2015) 1022–1027, <https://doi.org/10.1016/j.lwt.2015.07.033>.
- [15] S. Donkor, C. Larbie, G. Komlaga, B.O. Emikpe, Phytochemical, antimicrobial, and antioxidant profiles of *Duranta erecta* L. Parts, *Biochemistry Res. Int.* 2019 (2019), 8731595, <https://doi.org/10.1155/2019/8731595>.
- [16] Standards Press of China, Compilation of Chinese Forestry Standards-Forest Chemical and Specialty Products, ume, China Standards Press, Beijing, 1999.
- [17] L. Wang, Z. Ying, B. Sun, L. Tang, W. Du, W. Ge, C. Li, Optimization of processing technology of honey wheat bran based on Box-Behnken response surface methodology, *Chin. Tradit. Herb. Drugs* 52 (12) (2021) 3538–3543.
- [18] J. Meng, S. Xu, G. Lu, Optimization of ginger charcoal processing technology by central composite design response surface methodology, *Chinese J. Experiment. Prescript.* 18 (2) (2012) 8–11.
- [19] M. Valipour, M.E. Banihabib, S.M.R. Behbahani, Comparison of the ARMA, ARIMA, and the autoregressive artificial neural network models in forecasting the monthly inflow of Dez dam reservoir, *J. Hydrol.* 476 (2013) 433–441.
- [20] C.H. Kuo, T.A. Liu, J.H. Chen, C.M.J. Chang, C.J. Shieh, Response surface methodology and artificial neural network optimized synthesis of enzymatic 2-phenylethyl acetate in a solvent-free system, *Biocatal. Agric. Biotechnol.* 3 (3) (2014) 1–6.
- [21] M. Dadgar, S.M. Hosseini Varkiyani, A.A. Merati, Comparison between artificial neural network and response surface methodology in the prediction of the parameters of heat set polypropylene yarns, *J. Textil. Inst.* 106 (4) (2015) 417–430.
- [22] S.M. Huang, C.H. Kuo, C.A. Chen, Y.C. Liu, C.J. Shieh, RSM and ANN modeling-based optimization approach for the development of ultrasound-assisted liposome encapsulation of piceid, *Ultrason. Sonochem.* 36 (2017) 112–122, <https://doi.org/10.1016/j.ultrsonch.2016.11.016>.
- [23] P. Shao, S. Jiang, Y. Ying, Optimization of molecular distillation for recovery of tocopherol from rapeseed oil deodorizer distillate using response surface and artificial neural network models, *Food Bioprod. Process.* 85 (2) (2007) 85–92.
- [24] W. Tian, Z. Liao, J. Zhang, An optimization of artificial neural network model for predicting chlorophyll dynamics, *Ecol. Model.* 364 (2017) 42–52.
- [25] P. Kundu, V. Paul, V. Kumar, I.M. Mishra, Formulation development, modeling and optimization of emulsification process using evolving RSM coupled hybrid ANN-GA framework, *Chem. Eng. Res. Des.* 104 (2015) 773–790.
- [26] M. Aghbashlo, M.H. Kianmehr, T. Nazghelichi, S. Rafiee, Optimization of an artificial neural network topology for predicting drying kinetics of carrot cubes using combined response surface and genetic algorithm, *Dry. Technol.* 29 (7) (2011) 770–779.
- [27] S. Jacob, R. Banerjee, Modeling and optimization of anaerobic codigestion of potato waste and aquatic weed by response surface methodology and artificial neural network coupled genetic algorithm, *Bioresour. Technol.* 214 (2016) 386–395.
- [28] K. Ameer, S.W. Bae, Y. Jo, H.G. Lee, A. Ameer, J.H. Kwon, Optimization of microwave-assisted extraction of total extract, stevioside and rebudioside-A from *Stevia rebaudiana* (Bertoni) leaves, using response surface methodology (RSM) and artificial neural network (ANN) modelling, *Food Chem.* 229 (2017) 198–207.
- [29] E.G. Akhlu, A. Adem, R. Kasirajan, Y. Ahmed, Artificial neural network and response surface methodology for modeling and optimization of activation of lactoperoxidase system, *S. Afr. J. Chem. Eng.* 37 (2021) 12–22.
- [30] L.B. Bolzon, J.S. Dos Santos, D.B. Silva, E.J. Crevelin, L.A. Moraes, N.P. Lopes, M.D. Assis, Apigenin-7-O-glucoside oxidation catalyzed by P450-bioinspired systems, *J. Inorg. Biochem.* 170 (2017) 117–124.
- [31] S. Li, R. Yan, Y. Tam, G. Lin, Post-harvest alteration of the main chemical ingredients in *Ligusticum chuanxiong* Hort. (Rhizoma Chuanxiong), *Chem. Pharm. Bull.* 55 (1) (2007) 140–144.

- [32] S. Caporali, A. De Stefano, C. Calabrese, A. Giovannelli, M. Pieri, I. Savini, A. Terrinoni, Anti-inflammatory and active biological properties of the plant-derived bioactive compounds luteolin and luteolin 7-glucoside, *Nutrients* 14 (6) (2022) 1155.
- [33] Z. Lin, Y. Fang, A. Huang, L. Chen, S. Guo, J. Chen, Chemical constituents from *Sedum aizoon* and their hemostatic activity, *Pharmaceut. Biol.* 52 (11) (2014) 1429–1434.
- [34] Y. Liu, R. Wang, X. Liu, Y. Wang, M. Hou, Pb1989 short-term application of caffeic acid specifically promotes expansion of hematopoietic stem cells, *HemaSphere* 3 (S1) (2019) 901–902.